Theoretical study of sodium nitrite piezoelectricity and elasticity

2005 J. Phys.: Condens. Matter 17 4833

(http://iopscience.iop.org/0953-8984/17/30/009)

INSTITUTE OF PHYSICS PUBLISHING JOURNAL OF PHYSICS: CONDENSED MATTER

J. Phys.: Condens. Matter **17** (2005) 4833–4842 doi:10.1088/0953-8984/17/30/009

Theoretical study of sodium nitrite piezoelectricity and elasticity

M Catti[1], Y Noel[2] and R Dovesi[3]

[1] Dipartimento di Scienza dei Materiali, Università di Milano Bicocca, via Cozzi 53, 20125 Milano, Italy
[2] Laboratoire PMMP, Université Pierre et Marie Curie, 4 place Jussieu, 75252 Paris, France
[3] Dipartimento di Chimica IFM, Università di Torino, via Giuria 5, 10125 Torino, Italy

E-mail: catti@mater.unimib.it

Received 14 March 2005, in final form 13 June 2005
Published 15 July 2005
Online at stacks.iop.org/JPhysCM/17/4833

Abstract

The five piezoelectric stress coefficients e_{ik} of orthorhombic $Im2m$ $NaNO_2$ were calculated by *ab initio* quantum mechanical methods, employing the Berry phase theory, with an all-electron basis set of localized Gaussian-like functions and either a DFT-GGA or a Hartree–Fock Hamiltonian. DFT results are larger by about 30% than HF ones. The purely ionic and electronic contributions to piezoelectricity were evaluated by computing the internal and external (clamped-ion), respectively, components of each coefficient. In the e_{34} case the clamped-ion component is dominant, indicating that the electronic contribution prevails over the ionic one of opposite sign. In all other cases the overall piezoelectric effect is ruled by the ionic contribution. The full set of elastic constants was also computed, by means of which the piezoelectric strain coefficients d_{ik} could be derived. These are discussed and compared to experimental data from the literature.

(Some figures in this article are in colour only in the electronic version)

1. Introduction

Interesting prospects of calculating the piezoelectric properties of crystalline materials on the basis of a first-principles approach have been opened up by recent progress in theoretical insight and computational efficiency. In particular, the ambiguities which once affected the fundamental concept of polarization in periodic atomic systems were completely removed by the quantum mechanical theory based on Berry phases and presented about a decade ago [1, 2]. This may not only improve our fundamental understanding of the piezoelectric behaviour of solids, but also supplement somewhat the experimental techniques in this field. In fact, it is well known that the measuring of single crystal piezoelectric constants is severely hampered

by strict requirements on the quality of the sample, which has to be grown in a well controlled defect state.

A number of methods have been developed for calculating the piezoelectric properties of crystals. An early approach, based on linear response theory, provides the stress coefficients $e_{ik} = -(\partial\tau_k/\partial E_i)_\varepsilon$, which are derivatives of the stress components τ_k (Voigt's notation) with respect to the ith component of the electric field at constant strain ε. This method was implemented in computer codes based on a plane-wave expansion of the wavefunctions [3, 4]; second-order, non-linear effects cannot be simulated by this technique. In another scheme [5], the strain induced by application of a periodic electric field to the crystal is computed numerically, obtaining the piezoelectric strain coefficients $d_{ik} = (\partial\varepsilon_k/\partial E_i)_\tau$. In this case a supercell has to be built up, thus increasing the computational cost significantly. The third approach is based on the direct computation of the intensity of polarization $\boldsymbol{P}$ induced by strain by means of the Berry phase theory, so that the piezoelectric constants $e_{ik} = (\partial P_i/\partial\varepsilon_k)_E$ can be obtained by numerical differentiation. According to standard thermodynamics, $(\partial P_i/\partial\varepsilon_k)_E = -(\partial\tau_k/\partial E_i)_\varepsilon$ and $(\partial\varepsilon_k/\partial E_i)_\tau = (\partial P_i/\partial\tau_k)_E$. This method, implemented in the CRYSTAL computer code [6], proved to be successful for calculating the full piezoelectric tensors of ZnO and ZnS in their hexagonal wurtzite and cubic zinc blende phases [7], and it was used for the present work.

Molecular crystals may be much more challenging systems than simple close-packed inorganic structures for *ab initio* simulations of the piezoelectric behaviour, because more flexible and anisotropic chemical bonding is usually involved in crystal cohesion. This can produce a stronger structural relaxation under strain, requiring possibly a more demanding computational accuracy. Therefore we considered sodium nitrite, containing NO_2^- molecular ions with symmetrical triangular configuration and strong N–O covalent bonds, to be a good candidate for a study on this class of compounds. The room temperature ferroelectric phase of $NaNO_2$ has orthorhombic $Im2m$ symmetry, with the N and Na atoms lying on the y polar crystallographic axis. The spontaneous polarization of this phase has been characterized [8, 9], and its five independent non-zero d_{ik} piezoelectric coefficients have been reported [10]. On the other hand, no experimental e_{ik} values are available in the literature for $NaNO_2$. Two successive phase transitions from the ferroelectric to an incommensurate antiferroelectric phase at $T_c = 436.5$ K, and then to the paraelectric $Immm$ phase at $T_N = 438$ K, are observed. The paraelectric phase has a disordered crystal structure, resembling a superposition of the two ferroelectric orientation states [11].

Some preliminary results of this investigation, concerning the spontaneous polarization and the e_{ik} stress coefficients of sodium nitrite computed by the Hartree–Fock (HF) Hamiltonian, have been already reported [12]. The purpose of the present work is, first, to extend the calculation of the five e_{ik} piezoelectric constants by use of a density-functional-theory (DFT) Hamiltonian. The DFT technique is the most widely used in solid state simulations, and a full comparison with HF results for piezoelectric properties can be quite interesting. Further, we want to obtain the full set of elastic constants by both functionals, and to employ it for computing the d_{ik} strain coefficients, which can be compared to experimental results from the literature. Eventually, a decomposition of the e_{ik} values into their 'internal' and 'external' components will be carried out, so as to try to interpret the anisotropic piezoelectric effect of $NaNO_2$ in terms of the structural relaxation under mechanical strain.

2. Computational method

All quantum mechanical calculations were based on the periodic linear combination of atomic orbitals (LCAO) approach, where crystalline orbitals are expanded over basis sets

of localized functions (atomic orbitals). These are represented as products of radial functions (linear combinations of Gaussians) of the electron-to-nucleus distance times a real solid spherical harmonic. All-electron basis sets were employed for all atoms, with the following scheme of Gaussian contractions: 8(s)511(sp)1(d)G for Na, 6(s)311(sp)1(d)G for O, and 6(s)311(sp)1(d)G for N [12]; this corresponds to using 18 atomic orbitals to represent each of the three atoms. The self-consistent-field (SCF) equations for ground-state one-electron energy eigenvalues and eigenfunctions were solved both by Hartree–Fock (HF) and by density-functional-theory (DFT) Hamiltonians, according to the computational scheme implemented in the CRYSTAL03 computer code [6]. In the DFT case, a generalized-gradient-approximation (GGA) Perdew–Burke–Ernzerhof (PBE) functional [13] was used.

The level of numerical approximation in evaluating the Coulomb and exchange series appearing in the SCF equations for periodic systems is controlled by five tolerances [6]. These are related to estimates of overlap or penetration for integrals of Gaussian functions on different centres, which define cut-off limits for series summation. The values used in the present calculations are 10^{-7}, 10^{-7}, 10^{-7}, 10^{-7}, and 10^{-14}. The reciprocal space was sampled according to a regular sublattice defined by six points in the Monkhorst grid (46 points in the irreducible Brillouin zone). Convergence was checked with respect both to tolerances and to the number of Monkhorst points, and it was controlled by a threshold ($\Delta E = 10^{-9}$ Hartree per primitive unit cell) in the self-consistent-field cycles. In order to accelerate the SCF convergence, the level shifter technique was used: this enhances the energy difference between highest occupied and lowest empty states in the first cycles. Atomic coordinates were optimized by calculation of analytical gradients and subsequent conjugate gradient algorithm.

Polarization effects in insulating crystals can be computed, by the CRYSTAL03 code, either according to the Berry phase (BP) theory [1, 2] or by use of the Wannier function method. Concerning the first approach, the BP $\varphi_h^{(\varepsilon)}$ ($h = 1, 2, 3$) along the hth crystallographic axis, for the ε strain state of the crystal structure, is given by the following formula:

$$\varphi_h^{(\varepsilon)} = (2\pi V/|e|)\boldsymbol{P}\cdot\boldsymbol{a}_h^* = (V/4\pi^2)\sum_n \int \langle u_n(\boldsymbol{K})|-\mathrm{i}\boldsymbol{a}_h^*\cdot\nabla_{\boldsymbol{K}}|u_n(\boldsymbol{K})\rangle\,\mathrm{d}\boldsymbol{K}, \tag{1}$$

where V is the direct unit-cell volume, $|e|$ is the electron charge, $\boldsymbol{a}_h^*$ is the hth reciprocal lattice basis vector, n is the electron band index, $\boldsymbol{K}$ is the wavevector in the first Brillouin zone, and $u_n(\boldsymbol{x}, \boldsymbol{K}) = \psi_n(\boldsymbol{x}, \boldsymbol{K})\exp(\mathrm{i}\boldsymbol{K}\cdot\boldsymbol{x})$, where $\psi_n(\boldsymbol{x}, \boldsymbol{K})$ is the nth crystalline orbital (eigenfunction of the one-electron Hamiltonian). It is understood that all the $\boldsymbol{P}$, $\boldsymbol{a}_h^*$, V, and $u_n(\boldsymbol{K})$ quantities depend on the ε strain state of the crystal structure. Analogously to the polarization intensity $\boldsymbol{P}$, also the BP φ_h has no absolute physical meaning, but only its changes (e.g., those due to crystal strain) are defined and related to physical observables. It should be emphasized that equation (1) is quantum mechanically quite rigorous, so that the quality of the computed Berry phases depends only on the quality of the Bloch functions $u_n(\boldsymbol{x}, \boldsymbol{K})$ obtained by solving the SCF equations. This holds irrespective of the kind of chemical bonding present in the crystal considered.

By inverting the first equality in (1), the ith Cartesian component of the polarization intensity P_i can be derived as a linear combination of the BPs [14]:

$$P_i = (|e|/2\pi V)\sum_j a_{ji}\varphi_j, \tag{2}$$

where a_{ji} is the ith Cartesian component of the jth direct lattice basis vector $\boldsymbol{a}_j$. By differentiation one eventually obtains:

$$e_{ik} = (\partial P_i/\partial\varepsilon_k)_{\varepsilon=0} = (|e|/2\pi V)\sum_j a_{ji}(\partial\varphi_j/\partial\varepsilon_k)_{\varepsilon=0}. \tag{3}$$

Table 1. Unit-cell constants and free atomic fractional coordinates of $NaNO_2$ ($Im2m$ ferroelectric phase), optimized with the GGA-PBE and HF functionals and compared to experimental values.

a (Å)	b (Å)	c (Å)	V (Å^3)	y (Na)	y (N)	z (O)	
3.427	5.478	5.399	101.36	0.096 69	0.127 98	0.197 98	DFT-PBE
3.481	5.537	5.314	102.42	0.095 32	0.119 31	0.194 68	HF
3.502	5.521	5.379	104.00	0.088 3	0.122 8	0.196 5	Exp. (30 K) [15]
3.565	5.573	5.385	106.99	0.086 7	0.121 1	0.195 5	Exp. (298 K) [16]

Actually the three BPs $\varphi_j(\varepsilon_k)$ are computed by equation (1) as numerical functions of the strain parameter ε_k, from which the derivatives $\partial\varphi_j/\partial\varepsilon_k$ can be easily obtained. It should be stressed that, by use of equation (3), the *proper* piezoelectric stress coefficients are obtained, which do not depend on the arbitrary addition of lattice vectors times e/V to $\boldsymbol{P}$, and thus do not need correction terms equal to components of the spontaneous intensity of polarization $\boldsymbol{P}$ (cf [14] for a detailed explanation of this point).

In the case of $NaNO_2$, orthorhombic $Im2m$, one should be careful to use equation (3) because the computed BPs are referred to the primitive rather than to the body-centred unit cell, and thus the appropriate a_{ji} coefficients have to be used. The following expressions are obtained for the five independent piezoelectric constants:

$$\begin{aligned} e_{2k} &= (|e|/2\pi ac)(\partial\varphi_1/\partial\varepsilon_k + \partial\varphi_3/\partial\varepsilon_k - \partial\varphi_2/\partial\varepsilon_k) \qquad (k = 1, 2, 3), \\ e_{34} &= (|e|/2\pi ab)(\partial\varphi_1/\partial\varepsilon_4 + \partial\varphi_2/\partial\varepsilon_4 - \partial\varphi_3/\partial\varepsilon_4), \\ e_{16} &= (|e|/2\pi bc)(\partial\varphi_2/\partial\varepsilon_6 + \partial\varphi_3/\partial\varepsilon_6 - \partial\varphi_1/\partial\varepsilon_6). \end{aligned} \tag{4}$$

3. Results and discussion

3.1. DFT-GGA and HF stress piezoelectric tensors of $NaNO_2$

The origin on the polar axis was set as $y(\mathrm{O}) = 0$. Owing to symmetry constraints of the $Im2m$ space group, the only internal degrees of freedom are $y(\mathrm{N})$, $y(\mathrm{Na})$ and $z(\mathrm{O})$; the other fractional coordinates are $x(\mathrm{N}) = z(\mathrm{N}) = x(\mathrm{O}) = 0$, $x(\mathrm{Na}) = z(\mathrm{Na}) = 1/2$. Results of the structure optimizations with the DFT and HF Hamiltonians are reported in table 1, and therein compared to experimental data obtained at 30 [15] and at 298 K [16]. The agreement is good and in line with high-quality *ab initio* calculations: deviations of HF and DFT cell edges from corresponding 30 K data are within 1% and 2%, respectively, and atomic absolute coordinates show maximum shifts of a few 10^{-2} Å.

The piezoelectric stress coefficients were calculated by applying the five strains $[\varepsilon_1 00000]$, $[0\varepsilon_2 0000]$, and $[00\varepsilon_3 000]$ (range $-0.01 \leqslant \varepsilon_k \leqslant 0.01$) and $[000\varepsilon_4 00]$, $[00000\varepsilon_6]$ (range $-0.03 \leqslant \varepsilon_k \leqslant 0.03$) with 14 points computed for each deformation. In every case all free atomic coordinates were relaxed to find the least-energy structure configuration, and the three Berry phases φ_1, φ_2, and φ_3 were derived. Then the $(\partial\varphi_j/\partial\varepsilon_k)_{\varepsilon=0}$ derivatives were computed numerically, and the expressions (4) yielded the e_{ik} coefficients. The first three strains do not change the $Im2m$ space group, whereas in the other two cases the symmetry is lowered to monoclinic Cm. Only the (100) mirror plane is kept for the ε_4 strain, and there are thus six degrees of freedom (y and z coordinates of Na, N and O2, with y(O1) and z(O1) as origin-fixing values). In the ε_6 case, the (001) plane is retained with four free variables (x and y coordinates of Na and N, with x(O) and y(O) as origin-fixing values).

All calculations were performed both with the DFT-GGA-PBE and with the HF Hamiltonians. In the former case, we found an unexpected slow convergence of the results with

Table 2. Calculated (DFT-PBE and HF) piezoelectric stress coefficients e_{ik} (C m^{-2}) of $NaNO_2$, also decomposed into their internal $e_{ik}^{\rm int}$ and clamped-ion $e_{ik}^{(0)}$ contributions.

e_{21}	e_{22}	e_{23}	e_{34}	e_{16}	
−0.095	0.200	−0.147	0.150	−0.205	PBE: total
−0.069	0.114	−0.094	−0.420	−0.203	PBE: $e_{ik}^{\rm int}$
0.009	0.111	−0.034	0.683	0.015	PBE: $e_{ik}^{(0)}$
−0.104	0.089	−0.113	−0.533	−0.220	PBE: total − $e_{ik}^{(0)}$
−0.088	0.169	−0.104	0.132	−0.127	HF: total
−0.054	0.084	−0.056	−0.526	−0.130	HF: e_{ik}^{int}
−0.002	0.096	0.003	0.741	0.005	HF: $e_{ik}^{(0)}$
−0.086	0.073	−0.107	−0.609	−0.132	HF: total − $e_{ik}^{(0)}$

respect to the thickness of the grid used for the numerical integration of the electron density functionals. In order to obtain very stable and well converged e_{ik} values, a grid of '99/20' type [17] had to be used; with thicker grids, no more changes were observed in the results. These demanding computational conditions seem to be related to the peculiarly soft character of chemical bonding in sodium nitrite, as test calculations on ZnO attained convergence with a cheaper '75/16' grid.

The final results obtained are reported in table 2 (first lines). Small differences between the present HF results and the previous ones [12] are related to the more accurate structure optimization achieved in this work, which also produced a slightly different equilibrium geometry. The DFT values appear to be systematically larger (in modulus) than the HF ones, with the biggest difference (over 60%) for the e_{16} constant, and an average of about 20% for the other cases. The pseudo-symmetry $e_{21} \approx e_{23}$ and $e_{34} \approx -e_{16}$ already noticed for the HF results [12] seems to break down in the DFT case, suggesting, together with the larger spread of e_{ik} values, that a more anisotropic piezoelectric behaviour is predicted by DFT-PBE than by HF.

3.2. External and internal components of piezoelectric constants

A better insight into the ionic and electronic nature of piezoelectricity is given by considering every e_{ik} coefficient as the sum of $e_{ik}^{\rm int} = (\partial P_i/\partial \varepsilon_k)_{\varepsilon=0}$ and $e_{ik}^{(0)} = (\partial P_i/\partial \varepsilon_k)_x$ components due to pure internal (fixed unit cell) and external (fixed fractional atomic coordinates x) strains, respectively [18, 14, 7]. Such components account for the ionic ($e_{ik}^{\rm int}$) and electronic ($e_{ik}^{(0)}$) parts of the crystal relaxation under strain, giving rise to the total piezoelectric response. The internal piezoelectric constant can be expressed as follows:

$$e_{ik}^{\rm int} = \sum_s \sum_j (\partial P_i/\partial x_{sj})_{\varepsilon=0} (\partial x_{sj}/\partial \varepsilon_k)_{\varepsilon=0}$$
$$= (1/V) \sum_s \sum_j \left(\sum_{j'} a_{jj'} Z^*_{s,ij'} \right) (\partial x_{sj}/\partial \varepsilon_k)_{\varepsilon=0}, \qquad (5)$$

where the sums are extended over all atoms in the unit cell and over the three directions, and the quantities $Z^*_{s,ij} = V \partial P_i/\partial X_{sj}$ are the Born dynamical charge tensor components; x_{sj} and X_{sj} are the fractional and Cartesian, respectively, jth coordinates of the sth atom.

The internal and external components were calculated for all piezoelectric stress coefficients (table 2). In particular, the values of $e_{ik}^{\rm int}$ are compared to those of the $e_{ik} - e_{ik}^{(0)}$ differences: the relatively moderate discrepancies observed may be due to numerical errors

Table 3. Born effective charges $Z^*_{s,ij} = V(\partial P_i/\partial X_{sj})$ ($|e|$ units).

	$Z^*_{\mathrm{N},22}$	$Z^*_{\mathrm{Na},22}$	$Z^*_{\mathrm{N},33}$	$Z^*_{\mathrm{O},33}$	$Z^*_{\mathrm{N},11}$	$Z^*_{\mathrm{Na},11}$
PBE	0.262	1.072	2.303	−1.770	−0.150	1.005
HF	0.513	1.087	3.101	−2.154	0.000	0.950

Table 4. Derivatives $\partial x_{sj}/\partial\varepsilon_k$ for $NaNO_2$ (first lines, PBE; second lines, HF).

	$\partial/\partial\varepsilon_1$	$\partial/\partial\varepsilon_2$	$\partial/\partial\varepsilon_3$	$\partial/\partial\varepsilon_4$	$\partial/\partial\varepsilon_6$
x_{Na}					−0.158
					−0.126
x_{N}					0.179
					0.139
y_{Na}	−0.038	0.085	−0.054		
	−0.032	0.094	−0.033		
y_{N}	0.007	−0.101	0.014		
	0.007	−0.104	0.007		
z_{N}				−0.059	
				−0.059	
z_{O}				0.031	
				0.031	

introduced in the computation of equation (5), but also to a minor failure of the $e_{ik} = e^{(0)}_{ik} + e^{\mathrm{int}}_{ik}$ decomposition, because of small non-zero coupling terms between the internal and external components.

Let us first consider the behaviour of the e^{int}_{ik} components. The Born charges relevant for the five independent e_{ik} constants of $NaNO_2$, according to (5), were calculated and are reported in table 3. By comparison with formal atomic charges, it turns out that all the Na values are very close to +1 irrespective of the Cartesian direction and of the Hamiltonian used, as expected for a very ionic species. In all other cases, the values calculated by DFT-PBE are always lower than the HF ones, and then farther from ideal charges (cf the $Z^*_{\mathrm{O},33}$ case, where a full ionic behaviour is indicated by the HF result only). The nitrogen Born charges depend strongly on the crystallographic direction, always being much smaller than the formal value +5 and even getting vanishing or slightly negative in the $Z^*_{\mathrm{N},11}$ case.

The $(\partial x_{sj}/\partial\varepsilon_k)_{\varepsilon=0}$ quantities are reported in table 4. No substantial differences appear between DFT-PBE and HF results but for the ε_3 and ε_6 cases, where a slightly larger relaxation effect is shown by DFT-PBE data. Let us first consider the derivatives with respect to ε_1, ε_2 and ε_3: these control the internal parts of the e_{21}, e_{22} and e_{23} constants, which are related to changes of the P^{int}_2 (ionic) component of polarization intensity under strain. The total dipole moment arising from pure ionic displacements (internal part), projected along **b**, is related to the shortest $\overrightarrow{\mathrm{O–N}} \cdot \mathbf{b}$ and $\overrightarrow{\mathrm{O–Na}} \cdot \mathbf{b}$ distances (cf figures 1(a) and 2(a)); we then obtain per unit volume that $P^{\mathrm{int}}_2 = (2/ac)(Z^*_{\mathrm{N},22}y_{\mathrm{N}} + Z^*_{\mathrm{Na},22}y_{\mathrm{Na}})$, so that $e^{\mathrm{int}}_{2k} = \partial P^{\mathrm{int}}_2/\partial\varepsilon_k = (2/ac)(Z^*_{\mathrm{N},22}\partial y_N/\partial\varepsilon_k + Z^*_{\mathrm{Na},22}\partial y_{\mathrm{Na}}/\partial\varepsilon_k)$, which is the same formula as that given by (5). Now, it appears from table 4 that the signs of $\partial y_{\mathrm{N}}/\partial\varepsilon_k$ and $\partial y_{\mathrm{Na}}/\partial\varepsilon_k$ are always opposite, indicating that the relaxations of N and Na under strain have contrary effects on the polarization. However, as $Z^*_{\mathrm{N},22}$ is smaller than $Z^*_{\mathrm{Na},22}$, the relaxation of sodium prevails and dominates the internal piezoelectric response. The signs of the e^{int}_{2k} quantities (table 2) are thus the same as those of $\partial y_{\mathrm{Na}}/\partial\varepsilon_k$ (table 4).

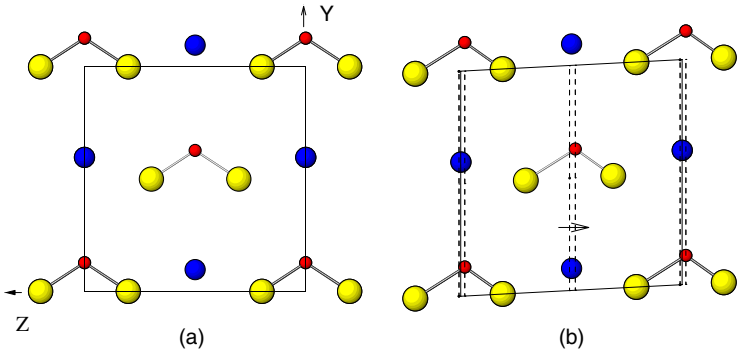

Figure 1. Projection onto the (100) plane of the equilibrium (a) and of the deformed ((b): e_{34} piezoelectric component, exaggerated distortion) crystal structures of $NaNO_2$. Small and large dark spheres represent N and Na atoms, respectively; pale spheres denote O atoms. The strain-induced internal polarization vector is shown in (b).

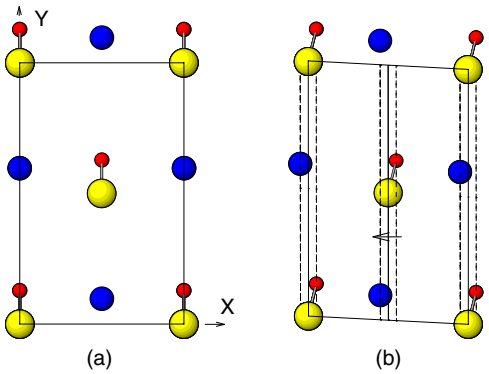

Figure 2. Projection onto the (001) plane of the equilibrium (a) and of the deformed ((b): e_{16} piezoelectric component, exaggerated distortion) crystal structures of $NaNO_2$. Small and large dark spheres represent N and Na atoms, respectively; pale spheres denote O atoms. The strain-induced internal polarization vector is shown in (b).

The $\partial z_N/\partial\varepsilon_4$ and $\partial z_O/\partial\varepsilon_4$ derivatives are relevant for the $e_{34}^{\rm int}$ quantity, according to (5): $e_{34}^{\rm int} = (2/ab)(Z^*_{N,33}\partial z_N/\partial\varepsilon_4 + Z^*_{O,33}\partial z_O/\partial\varepsilon_4)$. In this case not only the z derivatives but also the Born charges of N and O have opposite signs, so that an internal polarization along $-\boldsymbol{c}$ arises within the NO_2^- ion (figure 1(b)). As for the last internal piezoelectric constant, we have $e_{16}^{\rm int} = (2/bc)(Z^*_{N,11}\partial x_N/\partial\varepsilon_6 + Z^*_{Na,11}\partial x_{Na}/\partial\varepsilon_6)$. The situation is similar to that of the $e_{2k}^{\rm int}$ quantities, because N and Na relax into opposite directions (along the x instead of y axis in this case); however, here the $Z^*_{N,11}$ charge is vanishing (HF) or even negative (PBE), so that the contribution of N is either negligible or it adds to that of Na. A polarization along $-\boldsymbol{a}$, mainly contributed by the Na–O dipole, ensues (figure 2(b)).

All the $e_{ik}^{\rm int}$ values, as well as the clamped-ion contributions $e_{ik}^{(0)}$, are reported in table 2. The latter ones appear to be significant only in the e_{22} and e_{34}, and perhaps e_{23} cases. Further, it turns out that all the e_{ik} coefficients but e_{34} have the same signs as their corresponding internal components. This confirms the behaviour usually observed, e.g. in the ZnO and ZnS cases [7], that the major part of the piezoelectric effect is due to ionic relaxation. However, in the zinc chalcogenides the external components, though smaller in modulus than the internal ones,

Table 5. *Ab initio* (Hartree–Fock and DFT-GGA-PBE) values of elastic constants c_{hk} (GPa) and compliances s_{hk} (TPa^{-1}) for $NaNO_2$, compared to experimental data [21] linearly extrapolated to 0 K and to data measured directly at room temperature [20].

	DFT-PBE		HF		Exp.	
hk	c_{hk}	s_{hk}	c_{hk}	s_{hk}	c_{hk} (0 K)	c_{hk} (298 K)
11	43.3	35.9	46.3	29.3	38.8	31.7
22	85.8	13.4	75.7	15.4	78.9	58.2
33	94.6	16.0	97.9	12.9	86.4	66.0
12	20.6	−4.7	21.2	−6.0		12.6
13	36.5	−12.5	30.0	−7.6		19.7
23	27.0	−2.0	22.0	−1.6		17.4
44	18.7	53.5	17.6	56.8	17.2	12.4
55	4.7	212.8	9.9	100.7	9.5	9.9
66	4.2	238.1	9.1	110.0	5.2	4.8

always have the opposite sign, so that the purely electronic effect acts to reduce the magnitude of the ionic one. In $NaNO_2$, on the other hand, for e_{22} the internal and external components are both positive, whereas for e_{34} a very peculiar behaviour is observed: the two components have opposite signs, but the external one is larger in magnitude than the internal one. So, in this case the electronic contribution to piezoelectricity appears to prevail over the opposing ionic effect.

3.3. Elasticity and strain piezoelectricity

As the piezoelectric stress coefficients e_{ik} are not known from experiment, but the strain ones d_{ik} are [10], it is interesting for the purpose of comparison to derive the latter quantities indirectly from the e_{ik} values through the thermodynamic relationship:

$$d_{ik} = \sum_{h=1}^{6} e_{ih} s_{hk}, \tag{6}$$

where the s_{hk} quantities are the elastic compliance coefficients, components of the 6×6 (Voigt notation) **s** matrix which is the inverse of the **c** matrix of the elastic constants. In order to use this equation, the elastic constants $c_{hk} = (1/V)\partial^2 E/\partial\varepsilon_h \partial\varepsilon_k$ of sodium nitrite were calculated by applying the appropriate deformations and computing the second derivatives numerically. Full structural relaxations were always performed in all cases. A similar procedure was discussed in detail for the case of tetragonal MgF_2 [19].

The full set of elastic constants of $NaNO_2$ was obtained and reported in table 5, where it is also compared to experimental results by the Brillouin scattering method at room temperature [20], and to a partial set of values linearly extrapolated to 0 K from data measured by the ultrasonic pulse echo technique in the 293 to 473 K range [21]. The thermal effect is seen to be very large, so that extrapolating the data to the athermal condition is necessary; however, the resulting values are affected by some uncertainty, owing to the rather small temperature range used for the extrapolation. Both DFT-PBE and HF theoretical results agree satisfactorily with the extrapolated values from experiment; for the room-temperature extra-diagonal constants c_{12}, c_{13} and c_{23}, on the other hand, the discrepancy is obviously larger.

By inversion of the matrix **c** and using equation (6), the piezoelectric strain coefficients d_{ik} were computed and reported in table 6. Therein the values measured at room temperature by the resonance and antiresonance method [10] are also given. We observe a reasonable agreement

Table 6. Calculated and experimental [10] piezoelectric strain coefficients d_{ik} (pC N^{-1}) of $NaNO_2$.

d_{21}	d_{22}	d_{23}	d_{34}	d_{16}	
−2.5	3.4	−1.6	8.0	−48.8	PBE
−3.1	3.3	−0.7	7.0	−14.0	HF
−2.8	1.7	−1.2	9.3	−20.2	Exp.

between theory and experiment for the d_{21}, d_{23} and d_{34} constants, whereas the calculated d_{22} values are about double the measured data, and the PBE and HF d_{16} results are greatly over- and under-estimated, respectively, with respect to experiment. These discrepancies are not surprising, in view of the unknown thermal effect on the experimental d_{ik} values, and of the cumulative errors of the double calculation of the e_{ik} and c_{hk} quantities used to derive the theoretical d_{ik} strain coefficients.

4. Conclusions

The e_{ik} stress piezoelectric coefficients of $NaNO_2$ at the athermal limit were calculated successfully on the basis of the Berry phase theory. By use of the DFT-GGA-PBE Hamiltonian, larger absolute values are obtained than in the Hartree–Fock case, particularly for the e_{16} constant. This may be related to the Born dynamical charges being smaller with the PBE than with the HF functional. An insight into the microscopic origin of piezoelectricity in sodium nitrite could be given by comparing the internal (ionic) and external (electronic) components of the e_{ik} coefficients. In particular, the electronic contribution turned out to be negligible but for the e_{22} and e_{34} constants. In the e_{22} case, the ionic and electronic parts have the same sign and thus sum up, whereas they go into opposing directions for the e_{34} coefficient, with prevalence of the electronic effect. The full set of elastic constants was also calculated and employed, together with the e_{ik} results, to obtain the five d_{ik} strain piezoelectric coefficients at the athermal limit. A comparison with the room-temperature experimental data available from the literature is unfortunately biased by the strong thermal dependence of the elastic constants, and by the unknown corresponding effect for the d_{ik} quantities.

Acknowledgment

Financial support from MIUR-PRIN(COFIN), Rome, is acknowledged.

References

[1] King-Smith R D and Vanderbilt D 1993 *Phys. Rev.* B **47** 1651
[2] Resta R 1994 *Rev. Mod. Phys.* **66** 899
[3] de Gironcoli S, Baroni S and Resta R 1989 *Phys. Rev. Lett.* **62** 2853
[4] Hill N A and Waghmare U 2000 *Phys. Rev.* B **62** 8802
[5] Stahn J, Pietsch U, Blaha P and Schwarz K 2001 *Phys. Rev.* B **63** 165205
[6] Saunders V R, Dovesi R, Roetti C, Orlando R, Zicovich-Wilson C M, Harrison N M, Doll K, Civalleri B, Bush I J, D'Arco Ph and Llunell M 2003 *CRYSTAL03: User's Manual* (Italy: University of Torino) (UK: CLRC Daresbury Laboratory)
[7] Catti M, Noel Y and Dovesi R 2003 *J. Phys. Chem. Solids* **11** 2183
[8] Hamano K 1973 *J. Phys. Soc. Japan* **35** 157
[9] Buchheit W and Petersson J 1980 *Solid State Commun.* **34** 649
[10] Hamano K, Negishi K, Marutake M and Nomura S 1963 *Japan. J. Appl. Phys.* **2** 83

[11] Kay M I 1972 *Ferroelectrics* **4** 235
[12] Noel Y, Catti M and Dovesi R 2004 *Ferroelectrics* **300** 139
[13] Perdew J P, Burke K and Ernzerhof M 1996 *Phys. Rev. Lett.* **77** 3865
[14] Vanderbilt D 2000 *J. Phys. Chem. Solids* **61** 147
[15] Gohda T, Ichikawa M, Gustafsson T and Olovsson I 2000 *Acta Crystallogr.* B **56** 11
[16] Gohda T, Ichikawa M, Gustafsson T and Olovsson I 1996 *J. Korean Phys. Soc.* **29** 551
[17] http://www.crystal.unito.it/crystal03.pdf
[18] Dal Corso A, Posternak M, Resta R and Baldereschi A 1994 *Phys. Rev.* B **50** 10715
[19] Catti M, Pavese A, Dovesi R, Roetti C and Causà M 1991 *Phys. Rev.* B **44** 3509
[20] Shimizu H, Tsukamoto M, Ishibashi Y and Umeno M 1974 *J. Phys. Soc. Japan* **367** 498
[21] Hatta I, Shimizu Y and Hamano K 1978 *J. Phys. Soc. Japan* **44** 1887